STEM CELLS TRANSLATIONAL MEDICINE®

TISSUE ENGINEERING AND REGENERATIVE MEDICINE

Controlled Delivery of Stem Cell-Derived Trophic Factors Accelerates Kidney Repair After Renal Ischemia-Reperfusion Injury in Rats

HYUNG EUN YIM,[a,b,*] DOO SANG KIM,[a,c,*] HYUN CHUL CHUNG,[a,d,*] BRIAN SHING,[a] KYUNG HYUN MOON,[a,e] SUNIL K. GEORGE,[a] MICHAEL W. KIM,[a] ZACHARY ATALA,[a] JI HYUN KIM,[a] IN KAP KO,[a] JAMES J. YOO[a]

[a]Wake Forest Institute for Regenerative Medicine, Wake Forest School of Medicine, Medical Center Boulevard, Winston-Salem, North Carolina, USA; [b]Department of Pediatrics, College of Medicine, Korea University, Seoul, Korea; [c]Department of Urology, Soonchunhyang University Cheonan Hospital, Cheonan, Korea; [d]Department of Urology, Yonsei University Wonju College of Medicine, Wonju, Korea; [e]Department of Urology, Ulsan University Hospital, University of Ulsan College of Medicine, Ulsan, Korea

*Contributed equally

Correspondence: James J. Yoo, M.D., Ph.D., Wake Forest Institute for Regenerative Medicine, Wake Forest School of Medicine, Medical Center Boulevard, Winston-Salem, North Carolina 27157, USA. Telephone: 1-336-713-7294; e-mail: jyoo@wakehealth.edu

Received October 10, 2018; accepted for publication March 4, 2019; first published May 30, 2019.

http://dx.doi.org/10.1002/sctm.18-0222

Key Words. Acute kidney injury • Conditioned medium • Drug delivery systems • Kidney regeneration

ABSTRACT

Renal disease is a worldwide health issue. Besides transplantation, current therapies revolve around dialysis, which only delays disease progression but cannot replace other renal functions, such as synthesizing erythropoietin. To address these limitations, cell-based approaches have been proposed to restore damaged kidneys as an alternative to current therapies. Recent studies have shown that stem cell-derived secretomes can enhance tissue regeneration. However, many growth factors undergo rapid degradation when they are injected into the body in a soluble form. Efficient delivery and controlled release of secreting factors at the sites of injury would improve the efficacy in tissue regeneration. Herein, we developed a gel-based delivery system for controlled delivery of trophic factors in the conditioned medium (CM) secreted from human placental stem cells (HPSCs) and evaluated the effect of trophic factors on renal regeneration. CM treatment significantly enhanced cell proliferation and survival in vitro. Platelet-rich plasma (PRP) was used as a delivery vehicle for CM. Analysis of the release kinetics demonstrated that CM delivery through the PRP gel resulted in a controlled release of the factors both in vitro and in vivo. In an acute kidney injury model in rats, functional and structural analysis showed that CM delivery using the PRP gel system into the injured kidney minimized renal tissue damage, leading to a more rapid functional recovery when compared with saline, CM, or vehicle only injection groups. These results suggest that controlled delivery of HPSC-derived trophic factors may provide efficient repair of renal tissue injury. STEM CELLS TRANSLATIONAL MEDICINE *2019;8:959–970*

SIGNIFICANCE STATEMENT

The present study focuses on the development of an efficient delivery system that enables sustained release of human placental stem cell (HPSC)-derived conditioned medium (CM) for treatment of an acute kidney injury model using rats. The CM delivery using platelet-rich plasma (PRP)-based gel system into the injured kidney facilitated effective functional and structural restoration. These results suggest that the delivery of HPSC-derived trophic factors in a controlled manner may help efficiently repair renal tissue injury. The use of autologous PRP for the CM delivery into patients with kidney diseases will minimize possible side effects such as immune rejection.

INTRODUCTION

Increasing incidence of acute kidney injury (AKI) is contributing to the global health burden of chronic kidney disease (CKD) [1]. Although the pathogenic mechanisms of AKI have been elucidated in recent years, few preventive or therapeutic options exist [2]. Pharmacotherapeutic drugs have shown limited clinical efficacies in the treatment of AKI, highlighting a dire need of novel and innovative approaches [3, 4]. Recent advances in cell therapy have offered new therapeutic options for the treatment of kidney diseases [3–5]. Although the cell therapy approach has demonstrated promising outcomes in several preclinical and clinical studies, the practice of this approach remains a concern, as direct injection of the therapeutic cells can cause immune rejection, pulmonary embolism, and even teratoma formation in cases of pluripotent cells [6].

In an attempt to address the issues of cell therapy approach, several studies have shown that stem cell-derived secretomes can enhance tissue regeneration [7]. The use of cellular secretomes for therapy is an appealing alternative to cell transplantation. Secretomes have been used as a form of conditioned medium (CM), as a high level of growth factors and tissue repairing agents [7] from therapeutic cells are released into the culture medium. Numerous studies demonstrated positive outcomes of CM therapy in kidney diseases using various types of cells, including mesenchymal stem cells (MSCs) [8, 9] and induced pluripotent stem cells (iPSCs) [10]. However, the therapeutic effectiveness was obtained when highly concentrated CM was administered to appropriate delivery sites with high dose [10, 11]. For instance, Xing et al. [12] found that intravenous administration of MSC-CM did not improve the kidney function in an ischemia/reperfusion (I/R)-induced mouse injury model. This may be attributed to the intravenous injection without concentration of CM. In another study, Abedi et al. injected human MSC-CM intraperitoneally to the damaged kidney induced by gentamicin and observed partial tissue regeneration [13]. In either study [12, 13], the injected growth factors and cytokines present in the CM may lose their biological activity quickly because of the high diffusion rate and short half-life following injection [7, 14]. This may limit the time and dosage required to yield therapeutic effects. To overcome this limitation, controlled and sustained release of CM into the injured kidney is essential for achieving improved therapeutic efficacy [15].

Drug delivery systems have been developed to efficiently deliver biological factors to exert maximized outcomes in pharmaceutical applications and tissue regeneration [16–18]. Delivery vehicles, including natural and synthetic materials, have been designed to encapsulate target factors, thereby protecting them from the effect of enzymatic environment and prolonging therapeutic effects in vivo [16–18]. Therefore, the selection of the delivery vehicles is an important factor in controlling the biological activities of targeting molecules. In this study, we sought to develop an effective delivery system that provides controlled and sustained release of trophic factors to damaged cells and tissues.

We used platelet-rich plasma (PRP) gel as a delivery vehicle of CM. PRP is an easily accessible autologous source rich in growth factors and has shown healing efficacy in animal models and clinical studies [19, 20]. It can be easily manipulated as a gel system that allows efficient encapsulation of CM components. In our study, we used the CM secreted from human placental stem cells (HPSCs), as PSCs have features of both embryonic and MSCs, such as noncarcinogenic property and capability to differentiate into all three embryonic germ layers [21]. Placentas are usually discarded as medical waste after birth. Therefore, the use of these materials does not involve ethical issues. PSCs secrete many trophic factors that are involved in anti-inflammatory and immunomodulatory activities, angiogenesis regulation, cell proliferation, antiapoptosis, and antioxidative stress [22, 23]. Here, we evaluated the effects of trophic factors from HPSC-derived CM on renal regeneration. We examined the effects of HPSC-derived CM on cell proliferation and survival in vitro. To test the feasibility of controlled delivery, CM was physically encapsulated within the PRP and the release kinetics of CM from the gel was assessed. We evaluated the effects of PRP-encapsulated CM on the injured kidney using a rat AKI model.

Materials and Methods

Ethical Approval

The protocol for animal studies was approved by the Institutional Animal Care and Use Committee at the Wake Forest School of Medicine. All surgical procedures were carried out under the guidelines provided by the Institute for Laboratory Animal Research Guide for the Care and Use of Laboratory Animals. The authors took all steps to minimize the animals' pain and suffering.

Preparation of HPSC-CM

HPSCs were obtained from the Regenerative Medicine Clinical Center at the Wake Forest Institute for Regenerative Medicine [24]. HPSCs (passages 10–13) were grown in Dulbecco's modified Eagle medium (DMEM)/low-glucose media (GE Healthcare Life Sciences, Logan, UT) supplemented with 15% fetal bovine serum (FBS; Thermo Scientific, Carlsbad, CA), 18% Chang B (Irvine Scientific, Santa Ana, CA), 2% Chang C (Irvine Scientific), 1% L-glutamine, and 1% penicillin-streptomycin (GE Healthcare Life Sciences) at 37°C in 5% CO_2. Medium was changed every 2–3 days thereafter. To obtain HPSC-CM, HPSCs were plated at 1.5×10^6 cells per 15 cm culture dish and cultivated in the growth medium (GM) until the cells reached 60% confluence. Twenty milliliters of serum-free medium (SFM) without FBS and Chang C was added to the HPSCs and cultured for another 3 days. The approximate cell number at the time of the SFM addition was 5×10^6 cells per 15 cm culture dish. The CM was collected and filtered through a 0.22 μm filter. The CM was then concentrated by centrifugation using centrifugal filter units with a molecular weight cutoff of 3 kDa (Merck Millipore, Darmstadt, Germany). The concentrated HPSC-CM was stored at −80°C until use. For animal study, we used 80 μl of 10× concentrated CM to finally obtain 200 μl of 4× CM in the mixture with platelets and thrombin for injection (Table 1). The concentrated CM samples were analyzed for growth factor and cytokines content using the Quantibody human growth factor array (Ray-Biotech, Norcross, GA) [25].

Cell Culture and Hypoxic Treatment of Primary Renal Cells and Human Umbilical Vein Endothelial Cells

Isolation and culture of human-derived primary renal cell (PRCs) were previously established in our laboratory [26]. Briefly, PRCs were cultured in GM containing a mixture of an equal amount of two types of media. One was DMEM/high-glucose-containing 10% FBS and 1% penicillin-streptomycin and the second one was keratinocyte medium (Thermo Fisher Scientific, Rochester, NY) supplemented with bovine pituitary extract and epidermal growth factor; 1% FBS; 0.08% insulin-transferrin-sodium selenite (Sigma-Aldrich, St. Louis, MO); and 1% penicillin-streptomycin. Human umbilical vein endothelial cells (HUVECs) were purchased from Lonza (Walkersville, MD) and maintained in EGM-2 medium (Lonza). For hypoxic experiments, the cells were seeded into a 48-well plate or 8-well chamber slide (Thermo Fisher Scientific) at a density of 5,000 cells per well with GM, SFM, or HPSC-CM. Right after the cell seeding, the seeded cells were transferred in a hypoxia C-chamber (BioSpherix, Parish, NY) inside a standard CO_2 incubator (Revco Ultima II; Thermo Fisher Scientific) with a compact gas oxygen controller (ProOx P110; BioSpherix) to maintain

Table 1. Formulation of CM-PRP gels (total 200 μl injection per animal)

CM-PRP type	PRP/whole blood (μl/ml)	Platelet number ($\times 10^6$)	CM (μl of 10-fold conc.)	Thrombin (μl of 40 U/ml)
1	20/18	200	80	100
2	20/36	400	80	100
3	20/52	800	80	100

Abbreviations: CM, conditioned medium; PRP, platelet-rich plasma.

oxygen concentrations at 1% or 0.1% and 5% CO_2 for 3 or 7 days. Normoxic cells with GM, SFM, or HPSC-CM were incubated in a regular cell culture incubator with 21% O_2 and 5% CO_2. At the end of the study, cells were assessed morphologically and prepared for cell proliferation assays and immunofluorescent staining.

Cell Viability Assays

PRCs and HUVECs were seeded into 48-well plates at a density of 5,000 cells per well and treated with 0.25-, 0.5-, 1-, 2-, and 4-fold concentrated HPSC-CM for 1, 2, and 3 days. The cell viability was measured using Methods section (MTS) (Promega, Madison, WI) and phenazine methosulfate (PMS; Sigma-Aldrich) solutions. At the end of treatment, the culture medium was removed and 120 μl of the mixtures of MTS and PMS in SFM were added into each well and incubated at 37°C for 1 hour. The absorbance at 490 nm was measured using a microplate reader. Survival of PRCs and HUVECs was also assessed by a Live/Dead viability kit (Invitrogen, Carlsbad, CA) at 3 days after treatment. Briefly, the cells in 48-well plates were washed with phosphate-buffered saline (PBS) and incubated with a mixture of calcein AM (4 mM) and ethidium homodimer-1 (2 mM) at 37°C for 10–20 minutes. Then, fluorescent calcein (green, live cells) and ethidium homodimer-1 (red, dead cells) were visualized under a fluorescence microscope. To quantify the number of live cells, the live/dead stains were imaged in an ×200 magnification and the green fluorescent cells were counted (n = 3 images per group).

Immunofluorescence Staining of Cultured Cells

Cells grown on 8-well chamber slides (Thermo Fisher Scientific) were fixed with 4% paraformaldehyde for 10 minutes and permeabilized with 3% ice-cold methanol. The cells were then washed 3 times with PBS and incubated with primary antibodies against Aquaporin-1 (1:500; Abcam, Cambridge, UK), proliferating cell nuclear antigen (PCNA; 1:100; Santa Cruz, Santa Cruz, CA), and cleaved caspase-3 (1:200; Cell Signaling Technology, Beverly, MA) overnight at 4°C, followed by incubation with secondary goat anti-rabbit biotinylated IgG antibodies (1:300; Vector Laboratories, Burlingame, CA) for 30 minutes at room temperature. Subsequently, streptavidin conjugated with AF594 (1:200; Thermo Fisher Scientific) was added and incubated for 20 minutes at room temperature, followed by fluorescence microscopic imaging. The percentage of proliferating or apoptotic cells over the total cell number was calculated at a magnification of ×200 (100–400 cells, n = 3–5 per group).

Characterization of PRP Gel with HPSC-CM: Mechanical Analysis and CM Release Kinetics

PRP was isolated from porcine blood (Lumpire Biological Laboratories, Pipersville, PA) and mixed with CM and bovine thrombin (Sigma). Three PRP gels were formulated (Table 1) and their mechanical properties evaluated. Briefly, porcine blood was centrifuged at 400*g* for 10 minutes and then plasma and buffy coat in the supernatant were collected. The sample was centrifuged for 10 minutes at 800*g* and the PRP layer in the supernatant was collected. PRP, CM, and thrombin were mixed and kept for 1 hour at room temperature to allow for gelation before mechanical testing. The ratio of PRP to thrombin was determined based on a previous study reported in the literature [27], where the ratio of PRP/thrombin is 5 μl per unit. For comparison, PRP gels using 2.5 and 10 μl per unit were used for mechanical testing. Gels were characterized using an HR-2 Discovery Hybrid Rheometer (TA Instruments, Newcastle, DE) [25]. To initiate the measurement, the prepared gels were fixed on the rheometer stage and the surface of the gel was contacted with the 12-mm steel plate geometry. The rheometer program was configured to compress each gel sample until 0.4 N of axial force was achieved. Afterward, the rheometer performed an oscillatory stress sweep from 0.1 to 20 Pa to determine gel stiffness (storage modulus).

For the kinetic analysis of CM release, the CM was fluorescently labeled using 5-(and 6) carboxyfluorescein, succinimidyl ester N-hydroxysuccinimide (NHS)-fluorescein according to the manufacturer's instructions. Briefly, 1 ml of CM (approximately 1.5 mg/ml) was reacted with 10 μl of NHS-fluorescein on ice for 2 hours and then passed through a Sephadex G-10 (Sigma) column to remove the free NHS-fluorescein. To determine the labeling efficiency of proteins in the CM, BCA analysis was performed to measure the protein concentration of mixture of NHS and CM protein, and labeled CM proteins after the reaction. Approximately 56% of original CM proteins were identified in the labeled-CM samples. As the filtration with Sephadex G-10 column is efficiently able to remove the free NHS-fluorescein, most proteins in the CM are considered to be labeled with the fluorescein.

The fluorescent labeled CM was mixed with PRP and thrombin as described in Table 1 and incubated in PBS at 37°C. The released CM in the PBS was determined by measuring the fluorescent intensity at 488–520 nm using a microplate reader (SpectraMax M5). The percentage of accumulated CM release at each time point was determined by the ratio of fluorescent value at each time point to the total fluorescent intensity.

Animal Experiments

AKI was induced by I/R in rats as described previously by our group [28]. In brief, adult athymic nude male rats weighing 250–350 g (Charles River Lab, Wilmington, MA) were anesthetized with an intraperitoneal injection of sodium pentobarbital. A nontraumatic vascular clamp was placed across the renal artery and vein of both kidneys for 60 minutes. Then, the clamps were removed and reperfusion of the kidneys was confirmed visually. To test the effect of PRP-encapsulated HPSC-CM, the rats (n = 43) were divided into six groups, including age-matched control (AMC; n = 10), saline (n = 7), PRP (n = 6), CM (n = 7), HPSCs (n = 5), and CM with PRP (n = 8) groups. A

total volume of 200 μl of saline, PRP, CM, HPSCs (5×10^6 cells), or CM with PRP was injected into four sites of the kidneys (50 μl per site) immediately after I/R (Table 1). Blood samples were collected from the saphenous vein at 0, 1, 2, 3, 5, and 7 day after I/R, and serum Cr (Sigma) and neutrophil gelatinase-associated lipocalin (NGAL; BioPorto, Hellerup, Denmark) levels were analyzed using a NGAL enzyme-linked immunosorbent assay (ELISA) kit.

To track the delivery of CM encapsulated with PRP gels into the injured renal tissues, fluorescently labeled CM with or without PRP gel was injected into the kidney immediately after I/R injury. At 1 and 3 days after injection, the harvested kidneys were frozen and sectioned, followed by visualizing by immunofluorescent microscopy (Leica). At least, one image (×40 magnification) from a kidney was obtained from the injection site of the kidney. The fluorescent intensity was measured using the Image J software for semiquantification.

Morphology and Immunohistochemistry

To assess the histologic features of tubular injury resulting from renal I/R, paraffin-embedded sections (5 μm) of kidney tissue were stained with H&E and periodic acid-Schiff (PCH) stains using standard protocols. To evaluate the levels of acute tubular damage (n = 3–5 per each group), morphologic features were assessed in 10 fields of the cortex and outer medulla in cross-sections of the whole kidney using a semiquantitative scoring system (0–4). The percentage of total cortical tubules showing tubular cast formation, tubular dilatation, and tubular degeneration (vacuolar change, loss of brush border, detachment of tubular epithelial cells, and condensation of tubular nuclei) was estimated according to the following criteria under a light microscope (×200 magnification) by two blinded observers: 0, normal; 1, <25%; 2%, 25% to 50%; 3%, 50% to 75%; and 4, >75% of the relevant area. Immunohistochemistry was also performed to examine cell proliferation (PCNA), apoptosis (cleaved caspase-3), and peritubular capillaries (PTCs) density (JG12) in each group. The deparaffinized sections were heated in 0.01 M citrate buffer (pH 6.0; Polysciences, Warminster, PA) for 20 minutes, and endogenous peroxidase activity was neutralized with dual endogenous enzyme-blocking reagent (DAKO, Santa Clara, CA). The sections were incubated with primary antibodies at 4°C overnight. Primary antibodies against PCNA (1:100; Santa Cruz), cleaved caspase-3 (1:100; Cell Signaling Technology, Danvers, MA), and aminopeptidase P (JG12; 1:50; Santa Cruz) were used. The secondary antibodies were biotinylated anti-rabbit IgG antibodies (1:200; Vector Laboratories). The percentages of PCNA- and caspase 3-positive tubular cells in 10 fields of the cortex and outer medulla of the entire kidney cross-sections were determined under a light microscope (×200 magnification) by two blinded observers (n = 3–5 per each group). The nuclei colored in the dark brown or blue within the tubular structures were manually counted as positive or negative cells, respectively. The percentage of positive cells was determined from the ratio of positive cells to the total cells (positive and negative cells).

PTC loss was determined as the percentage of the area with no capillaries stained with JG12 antibody, which was formerly reported as a rarefaction index of PTC sparseness [29]. Briefly, this index was calculated via counting the total number of squares in 10 × 10 grids that did not show JG12-positive PTC staining in randomly selected 10 non-overlapping fields (×200 magnification). The lowest PTC rarefaction index is 0, that is, all squares in the grid contain JG12-positive PTCs, whereas the highest score is 100, that is, JG12-positive PTCs are absent from all squares in the grid (n = 3–5 per each group).

Renal Injury Marker Quantification in Whole Kidney

To determine the level of renal tissue injury, we quantified the total protein levels of NGAL, KIM-1, cystatin C, and casapse-3 by ELISA in whole kidneys obtained from all experimental groups 7 days post-I/R injury. Each marker level was measured in duplicates by sandwich ELISA techniques using commercially available rat NGAL (Enzo life science), KIM-1, cystatin C (Abcam), and caspase-3 (Mybiosource, San Diego, CA) immunoassay kits according to the manufacturer's instructions.

Statistical Analysis

Data are presented as mean ± SD. Statistical comparisons between groups were analyzed using one-way ANOVAs and t tests as appropriate. Tukey's post hoc analysis was used for multiple comparisons when appropriate. A p value <.05 was considered significant. Statistical analyses were performed with SPSS ver. 16.0 for Windows software (SPSS Inc., Chicago, IL).

Results

HPSC-Derived CM Enhances Cell Proliferation and Survival in a Dose-Dependent Manner

To determine the effect of HPSC-derived CM on cell proliferation and survival, human PRCs and HUVECs were treated with 0.25 to 4-folds concentrated up to 3 days and cell viability and survival determined using MTS and live/dead cell assay, respectively. As shown in Figure 1A, 1C, treatment of PRCs and HUVECs with HPSC-derived CM induced a significant increase in cell viability in a dose-dependent manner. Live/dead cell staining was conducted at day 3 of culture. The number of dead cells was significantly reduced in both PRCs and HUVECs treated with higher CM concentrations (Fig. 1B, 1D; Supporting Information Fig. S1).

To determine the effect of CM on cellular behaviors under hypoxic conditions, cells were cultured under low oxygen conditions for 3 days and stained with PCNA and cleaved caspase-3 antibodies. PCNA staining revealed that CM treatment increased the proportions of proliferating PRCs (Fig. 2A, 2B) and HUVECs (Fig. 2E, 2F) under both normoxic (21%) and hypoxic conditions (1% and 0.1%; *p < .05) at 3 and 7 days of culture (Supporting Information Fig. S2A). Particularly, an increased PCNA expression was quantitatively confirmed by ELISA (*Student's t test, p < .05, n = 4) and Western blot (Supporting Information Fig. S3). CM treatment significantly reduced the number of apoptotic cells at 3 (Fig. 2C, 2D, 2G, 2H; *p < .05) and 7 days (Supporting Information Fig. S2B; p < .05). Under both normoxia and hypoxia, PRCs maintained their renal phenotypes in the presence of CM, as confirmed by AQP1 immunoreactivity (Supporting Information Fig. S4).

The Release of PRP Gel-Encapsulated CM In Vitro and In Vivo

To determine the release kinetics of CM from PRP gel, fluorescent-labeled CM was encapsulated into various

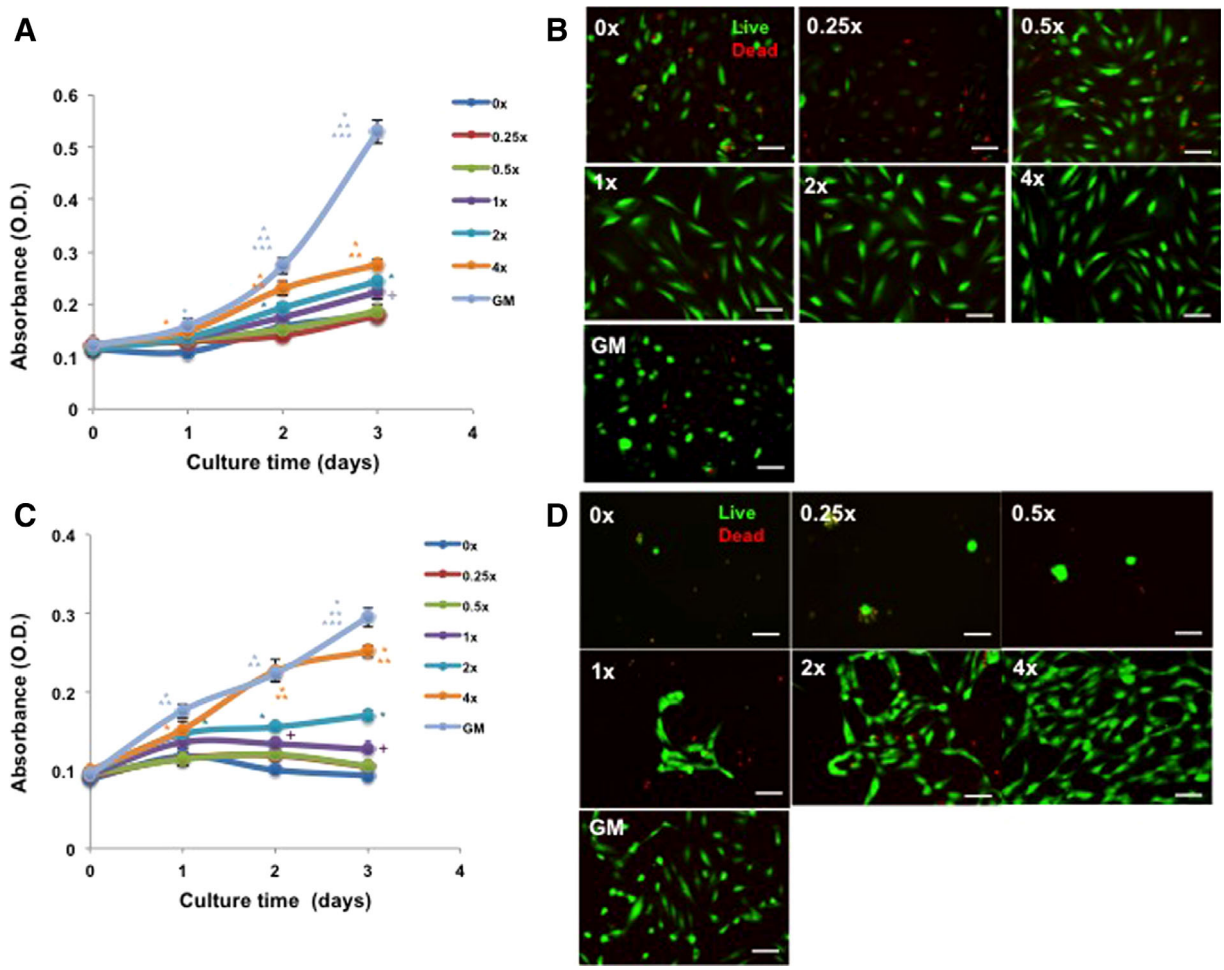

Figure 1. Human placental stem cell (HPSC)-derived conditioned medium (CM) improves cell viability and proliferation. HPSC-CM resulted in concentration-dependent increases of cells in proliferation for both renal (primary renal cells [PRCs]; **A**) and endothelial cells (human umbilical vein endothelial cell [HUVEC]; **C**) at 1, 2, and 3 days (analysis of variance, Tukey post hoc analysis at $p < .05$; **(A)** 1 day [*, with 0×], 2 and 3 day [*, with 0×, 0.25×, 0.5×, 1×; **, with 2×; ***, with 4×; +, with 0×, 0.25×, 0.5×]; **(C)** *, with 0×, 0.25×, 0.5×, 1×; **, with 2×; ***, with 4×; +, with 0×; $n = 3$). Viable cells (green) were prominent in the CM-treated groups in a concentration-dependent manner at 3 days for both PRC (**B**) and HUVEC (**D**) (0-, 0.25-, 0.5-, 1-, 2-, and 4-fold; ×200, Bar = 100 μm). Dead cells fluoresce red. As a positive control, cells were also cultured with respective normal GM. Abbreviation: GM, growth medium.

concentrations of PRP gels (Table 1) and the release kinetics of CM were determined by CM-derived fluorescent intensity. Mechanical testing using a rheometer showed that the stiffness of the PRP gel increased with increased numbers of platelets (Fig. 3A). The release rate of CM depended on the gel stiffness (Fig. 3B). Based on these results, a PRP gel (400×10^6 platelets) with moderate release of CM was chosen for the subsequent studies. We injected CM and PRP-encapsulated CM into rat kidneys and harvested the tissues at 24 and 72 hours postinjection. At 24 hours postinjection, the fluorescence intensity of the kidney injected with PRP-encapsulated CM was much higher than that of the CM without encapsulation (Fig. 3C, 3D), indicating that the PRP gel system can control the sustained release of CM in vivo.

Amelioration of Renal Function by the PRP-Encapsulated CM

To determine the effect of PRP-encapsulated CM on injured kidneys, we created AKI in male athymic rats by I/R. 200 μl of saline, PRP, CM, HPSCs (5×10^6 cells), or PRP-encapsulated CM (CM + PRP) were injected into the kidneys immediately after I/R. Serum creatinine (Cr) and NGAL levels were analyzed at days 0, 1, 2, 3, 5, and 7 after injury. Serum Cr and NGAL levels were significantly higher in the rats received I/R, compared with the untreated normal rats (Fig. 4). Serum Cr levels in the AKI rats that received PRP-encapsulated CM injection were significantly lower than those in all other groups at day 1 (ANOVA, Tukey post hoc test at $*p < .05$) and consistently maintained low levels during the remaining testing period (Fig. 4A). Similarly, serum NGAL levels in the CM + PRP group were significantly reduced based on the ANOVA and Tukey post hoc test ($*p < .05$), at 3, 5, and 7 days post-treatment, as compared with the saline injection group (Fig. 4B). Also, the serum NGAL level of the CM only (**) and HPSC injection (***) groups is significantly different from that of saline group at day 7.

We performed histological and immunohistochemical analyses on the kidney tissues to further analyze the I/R-induced AKI. H&E staining showed that the tubular dilation in the CM-PRP-treated group was significantly reduced when compared

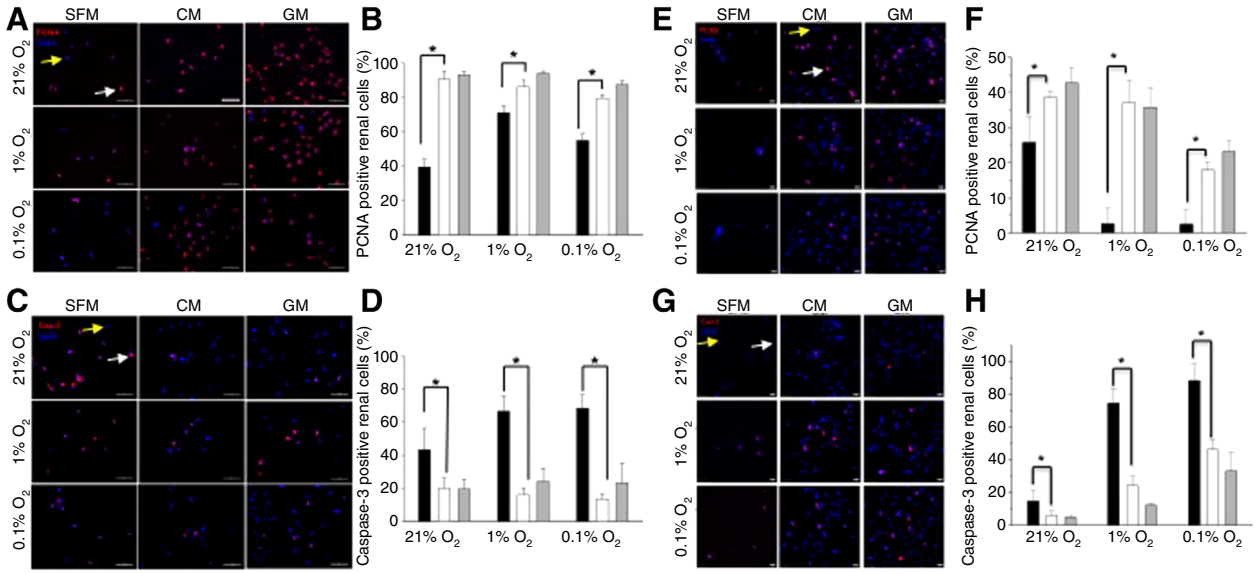

Figure 2. Treatment with human placental stem cell **(**HPSC)-derived conditioned medium (CM) for 3-day culture reduces cell apoptosis and enhances cellular proliferation. Representative immunofluorescent images demonstrate that more PCNA positive cells (**A, B** for primary renal cell [PRC]; **E, F** for human umbilical vein endothelial cell [HUVEC]) and fewer cleaved caspase-3 staining (**C, D** for PRC; **G, H** for HUVEC) cells were found in CM-treated groups versus SFM-treated groups. Positive effects of HPSC-CM treatment on cellular behaviors were evident irrespective of oxygen concentration (Student's *t* test, **p* < .05; SFM vs. CM; black bar, SFM; white bar, CM; gray bar, GM). Data presented as mean ± SD (*n* = 100–400 cells from three different experiments; ×400 magnification, Bar = 50 μm **(A, C)** and 20 μm **(E, G)**). Four-fold concentrated CM was used in all experiments; cells were also grown under normal GM as positive controls. White and yellow arrows indicate positive and negative for each marker, respectively. Abbreviations: CM, conditioned medium; GM, growth medium; PCNA, proliferating cell nuclear antigen; SFM, serum-free medium

with the other groups (**p* < .05) (Fig. 5A). PAS staining indicated that the brush border (arrow head) loss in proximal tubules was also significantly reduced in the CM-PRP group than those in other groups (**p* < .05; Fig. 5B). In addition, CM-PRP treatment enhanced renal cell proliferation and diminished renal cell apoptosis (**p* < .05) **(**Fig. 6A, PCNA, and 6B, caspase-3). These results demonstrate that delivery of CM with PRP efficiently reduced I/R-induced tubular damage.

To further evaluate the improvement of renal functions, protein expression of renal damage markers including NGAL, KIM-1, cystatin C [30], and caspase-3 [31] was determined. Figure 7 shows that the level of each marker significantly increased after I/R injury and saline treatment. Interestingly, all of treatments significantly reduced the level of each marker with a statistical difference (ANOVA, $p < .0001$, *, Tukey post hoc test at $p < .05$ with saline). Additionally, CM only, HPSC, and CM + PRP treatment significantly reduced the apoptosis-related marker, caspase-3 protein, as compared with that of the PRP treatment group (ANOVA, $p < .0001$; *, Tukey post hoc test at $p < .05$, *, with saline, and **, with PRP).

Another histologic feature of renal I/R is loss of PTC. We stained the kidney sections with JG12, a membrane antigen presented on rat endothelial cells. PTC loss was calculated as the percentage of the area without positive staining of JG12 and expressed as PTC rarefaction index. I/R treatment resulted in a significant increase in PTC rarefaction score. The changes in PTC loss in the treatment groups were consistent with the renal tubular injury score and renal cell apoptosis. The PTC rarefaction index scores from the CM-CRP (**p* < .05) and HPSC (***p* < .05) treatment groups were significantly lower than those from saline-treated, PRP-treated, and CM-only-treated rats (Supporting Information Fig. S6A, S6B). Of note, the level of endogenous vascular endothelial growth factor (VEGF) protein was higher in the kidney tissues treated with CM-PRP than those in saline-treated, PRP-treated, and CM-only-treated rat kidneys (Supporting Information Fig. S6C; *, ***p* < .05). No significant changes in renal hepatocyte growth factor (HGF) were observed among the treatment groups (Supporting Information Fig. S6D**)**.

Discussion

To date, no treatment modalities are able to change the outcomes of AKI in patients. Although recent studies indicate that cell-based therapies have potential in treating AKI [3, 4, 8, 9], there are still many obstacles to overcome [4, 6]. Preclinical data show that cell-secreted factors can mitigate renal injury such as AKI [10], but a well-controlled delivery system is needed to achieve maximized beneficial outcomes. To this end, the aim of this study was to develop a delivery system for HPSC secretomes in order to efficiently control the release of secretory molecules into the affected kidneys, thereby restoring kidney function.

Our results indicate that the controlled delivery of HPSC-CM using a PRP gel appeared to be an effective approach in facilitating functional and structural recovery of the kidney from I/R injury. Tarng et al. [10] examined the effects of iPSC-derived CM on renal improvement in a rat model of I/R. The renal improvement was only observed in the treated group with 50-fold concentrated CM (a total of 4 ml). In another study using a rat model of CKD, van Koppen et al. found that

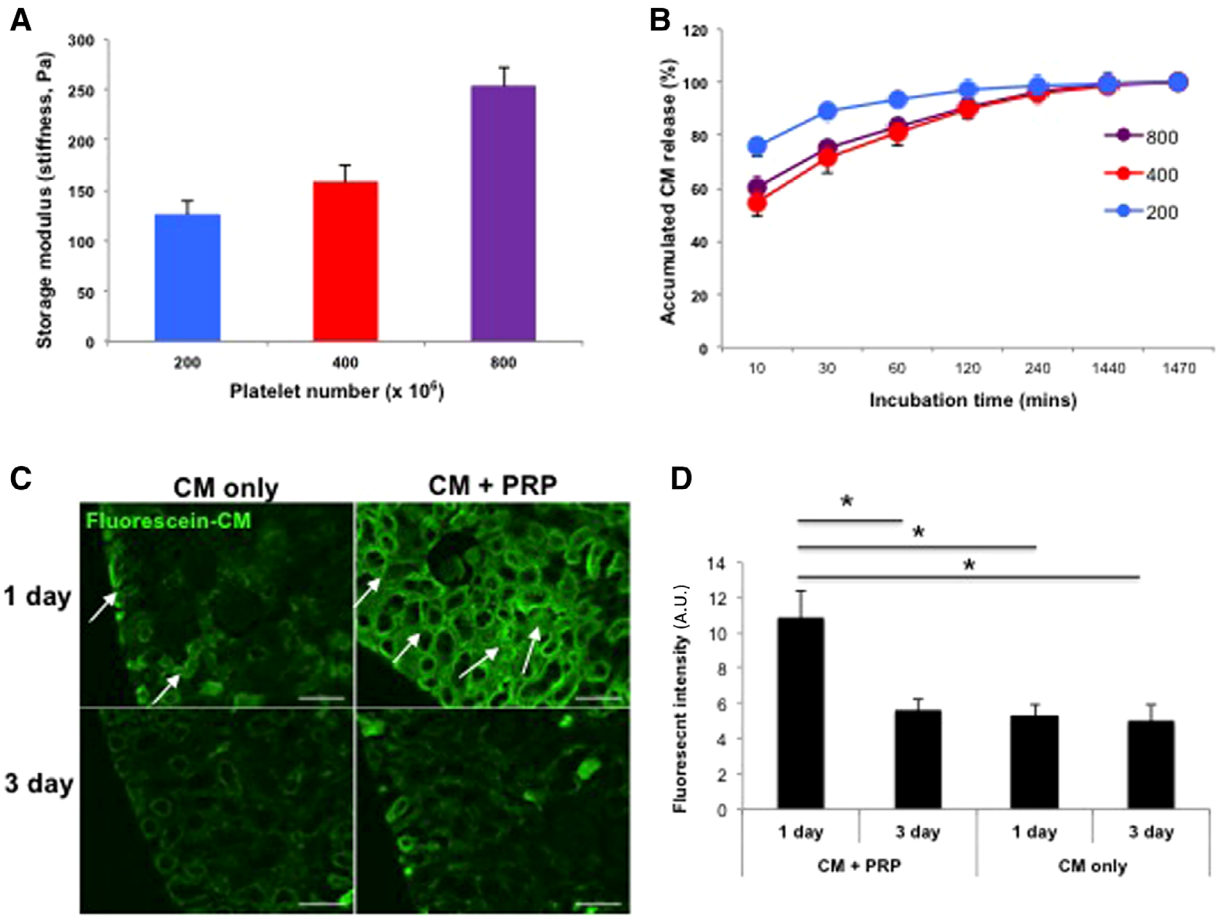

Figure 3. Controlled release of CM from PRP gel in vitro and in vivo. **(A):** Mechanical stiffness of PRP gels increased with increased concentrations of platelets (n = 3 per sample). **(B):** Sustained release of CM from all PRP gels was detected over 24 hours, and stiffer gels (400 and 800 × 10^6 platelets) released CM more slowly. Based on these results, PRP with 400 × 10^6 platelets were chosen for all further experiments. **(C):** Fluorescently labeled CM encapsulated in the PRP gel was localized to cortex region (arrows) at 1 day after ischemia/reperfusion, whereas CM without PRP quickly disappeared. In both groups, intensity of green fluorescence gradually decreased up to 3 days. **(D):** Semiquantitative analysis for fluorescent intensity showed more effective delivery of CM with PRP gel than CM-only injection at 1 day postinjection (*p < .05). Data presented as mean ± SD (n = 2 animals, four kidneys per experimental group; ×200 magnification, Bar = 100 μm). Abbreviations: A.U., arbitrary units; CM, conditioned medium; PRC, primary renal cell.

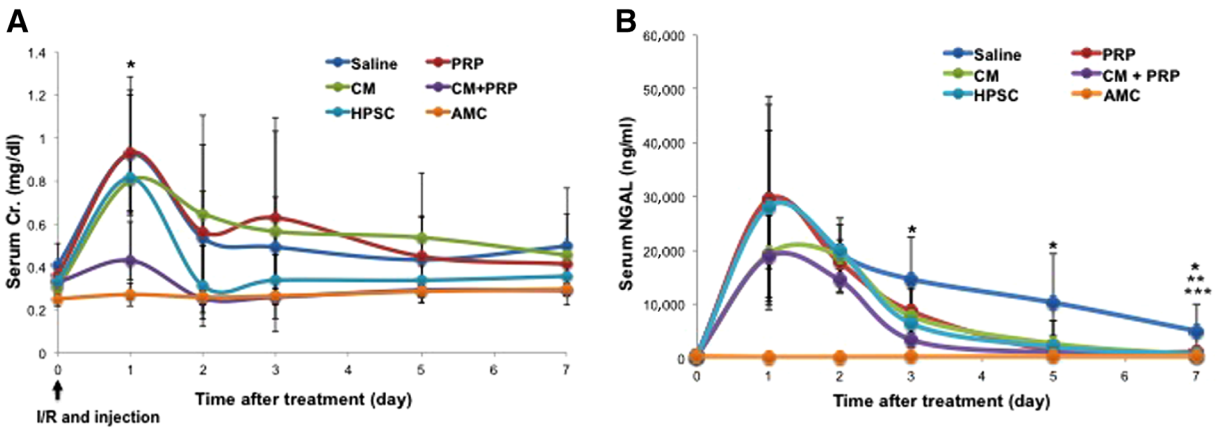

Figure 4. Functional improvement by injection of HPSC-CM encapsulated with PRP in rats after ischemia/reperfusion (I/R). **(A):** Serum Cr levels in the CM with PRP group (CM + PRP) were significantly lower than in saline-treated, PRP-only-treated, and CM-only-treated groups at 1 day post-I/R (analysis of variance, Tukey test, *p < .05, CM + PRP vs. saline, PRP only, and CM only, n = 3–6). Although similar elevations in serum NGAL levels were observed, renal function improved the most in the CM + PRP group, based on lower serum NGAL levels than in the saline group at 3, 5, and 7 days (*, Tukey test at p < .05, CM + PRP vs. saline). **(B):** NGAL levels in the CM only and HPSC group also significantly decreased, compared with the saline group at 7 days (Tukey test at p < .05; **, CM vs. saline; ***, HPSC vs. saline). Data presented as mean ± SD (n = 3–6 per experimental group). Abbreviations: AMC, age-matched control; CM, conditioned medium; HPSC, human placental stem cell; NGAL, neutrophil gelatinase-associated lipocalin; PRP, platelet-rich plasma.

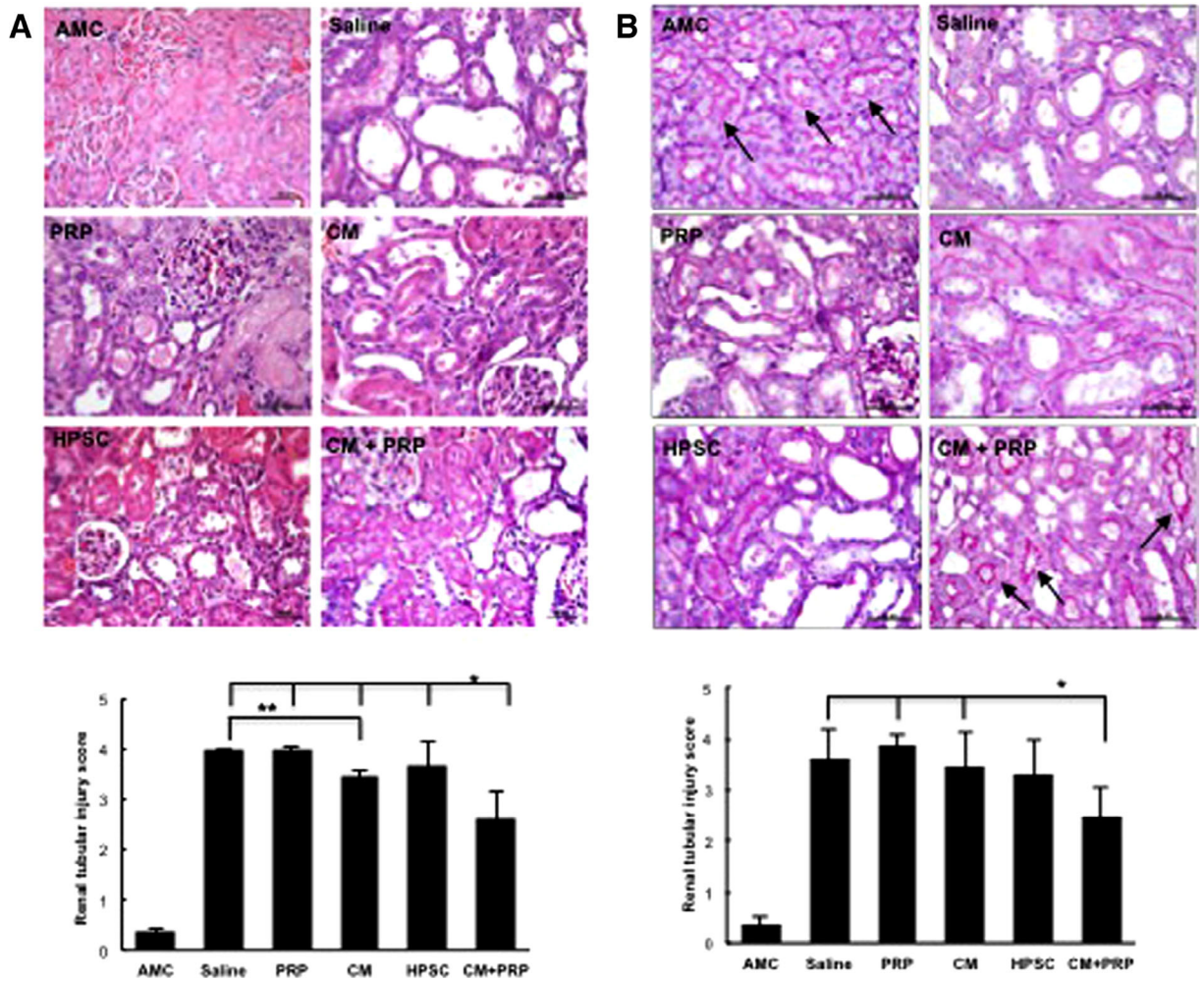

Figure 5. Structural amelioration of renal tubular injury in the HPSC-CM encapsulated with PRP group. Representative images with **(A)** H&E or **(B)** periodic acid-Schiff staining (PAS images) and semiquantitative analyses of renal tubular injury in all treatment groups at 7 days post-ischemia/reperfusion. Tubular injury was improved CM with PRP (CM + PRP). Renal tubular injury scores obtained from H&E-stained tissues were lowest in the CM with PRP group, compared with all other treatment groups (analysis of variance [ANOVA], Tukey test, $^{*}p < .05$ vs. all other treatments). In the H&E-stained tissues, the CM group also showed a lower tubular injury score than the saline group (ANOVA, Tukey test, $^{**}p < .05$ vs. saline) **(A)**. In the PAS-stained tissues, the brush border in proximal tubules (arrows) was relatively preserved by CM + PRP, and tubular injury scores in the CM + PRP group were lower than those of the saline, PRP, and CM groups (ANOVA, Tukey test, $^{*}p < .05$ vs. saline, PRP, and CM groups) **(B)**. Data presented as mean ± SD (n = 3–5 per experimental group). Scale bar = 50 μm. Abbreviations: AMC, age-matched control; CM, conditioned medium; HPSC, human placental stem cell; PRP, platelet-rich plasma.

human embryonic MSC-derived CM decreased the progression of CKD and improved tubular and glomerular injury [11]. As in the case of the study [10], a high dose of CM injection (2 ml of 25 times concentrated of CM) was required to obtain an effective outcome [11]. Intravenous injection of non-concentrated CM (a total of 3.5 ml) did not restore renal function in a mouse I/R model [12].

In contrast, we injected 200 μl of 10-times concentrated PRP-encapsulated CM (CM + PRP) into four different sites of both kidneys with 50 μl volume per injection and observed significant improvement in renal function (Fig. 4), histologic analysis (Figs. 5–6), and the level of renal damage (Fig. 7). The effective HPSC-CM dose used in our studies is much lower than that used in other studies above [10, 11] by a 25- or 100-fold in the injected volume of CM. As shown in the results, the reduction of serum Cr and NGAL by the CM + PRP group is significantly different from that observed by the saline injection, which is confirmed by histological analysis and renal damage (Figs. 5–7**)**. Also, the experimental evidences support that the therapeutic effect by the CM + PRP delivery is significantly different from the PRP only group (Figs. 5–7). As positive control, HPSC injection facilitated therapeutic effects on the improvement of renal functions as similar level as that by CM + PRP treatment. Interestingly, the beneficial phenomenon was observed at the later time points (e.g., 7 days) post-treatment (Fig. 4B). This delay in the therapeutic effects may be because of the time required for cell engraftment after the HPSC injection and additional time frames for the grafted cells to play roles to ameliorate the renal damage. In addition, determination of the renal damage level on the harvested tissue demonstrated that NGAL, cystatin C, and caspase-3 level is similar to that of the CM + PRP group and the effects are statistically significant as compared to the control (saline). Moreover, in the comparison of beneficial effect between the CM

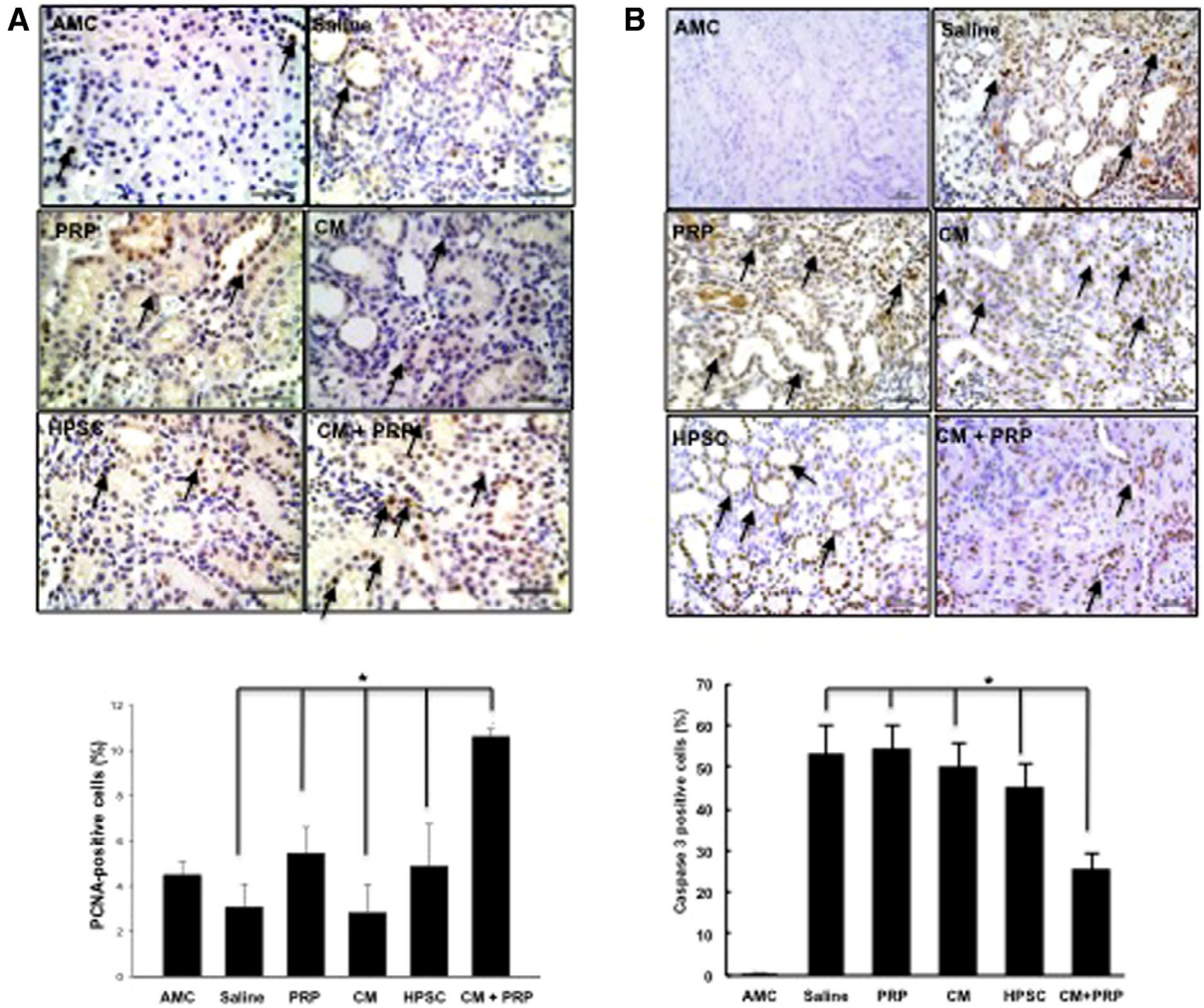

Figure 6. Enhanced cell viability by treatment of HPSC-CM with PRP. Representative images and semiquantitative analysis for renal cell proliferation (**A**; PCNA staining) and renal cell apoptosis (**B**; cleaved caspase-3 staining) demonstrated cellular viability and proliferation of renal cells within the tubular structures. PCNA-positive staining (brown nuclear spots, arrows) was greater in the CM with PRP group than all other treatment groups and AMC (analysis of variance [ANOVA], $^{*}p < .05$ vs. all) **(A)**. Renal cell apoptosis confirmed by caspase-3 staining was diminished by treatment of CM with PRP (ANOVA, $^{*}p < .05$, vs. all other treatments) **(B)**. Data presented as mean ± SD (n = 3–5 per experimental group). Scale bar = 50 μm. Abbreviations: AMC, age-matched control; CM, conditioned medium; HPSC, human placental stem cell; PCNA, proliferating cell nuclear antigen; PRP, platelet-rich plasma.

+ PRP and the CM only treatment, the improvement of therapeutic outcomes in the CM + PRP group appears to be superior to that of the CM-only delivery while the CM only treatment group also showed the beneficial effects on the renal damages, as observed in the functional and histological analysis (Figs. 4–7). The significant difference between the two groups was confirmed in the serum Cr level (Fig. 4A) at very early time point (1 day) post-treatment and CM only treatment ameliorated renal damages as observed in the functional and histological analysis (Fig. 4–7). The significant difference can be found in the serum Cr level (Fig. 4A) at 1-day post-treatment and histological analysis (Fig. 6) with a statistical difference (ANOVA, Tukey post hoc test at $p < .05$, *CM + PRP vs. CM only). This outcome implies the importance of sustained release of CM from the PRP-encapsulated CM from the injection site, which was confirmed by the in vivo release test (Fig. 3C, 3D). Since the previous studies used various kidney injury models (e.g., AKI and CKD), CM sources (iPS-CM and MSC), and administration routes (intraperitoneally and intravenously) [10, 11], it makes direct comparisons very difficult. However, the dose that we used in our studies was much lower than that used previously, implying that effectively controlled CM delivery appears to be an important requisite for mitigating renal injuries. It will be interesting to see whether increasing the CM-PRP dosage can obtain better therapeutic outcomes.

As mentioned in other studies [10, 11, 32], the potential mechanisms involved in the therapeutic effect of HPSC-CM in the AKI model may be because of the renoprotective effects of the delivered CM within the injured kidneys. Previous studies have reported that the therapeutic effects by CM treatment primarily occurred via attenuation of cellular apoptosis through protection from the reactive oxygen species [10] as well as kidney regeneration [11, 32] through angiogenesis and tubular regeneration. Our study also demonstrated similar phenomena in the CM treatment, both in vitro and in vivo.

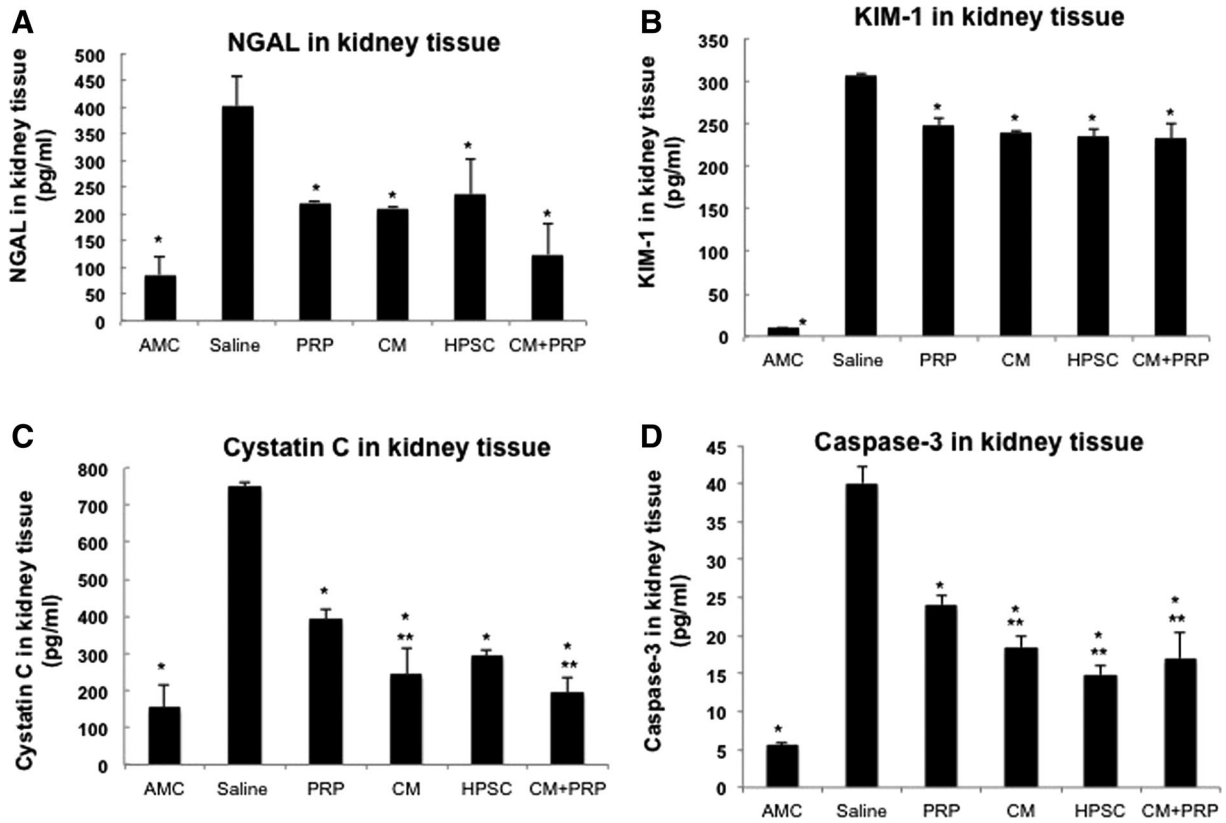

Figure 7. Amelioration of acute kidney injury-derived renal damages by therapeutic treatments. The levels of **(A)** NGAL, **(B)** KIM-1, **(C)** cystatin C, and **(D)** caspase-3 in the harvested kidney post-treatment were determined by enzyme-linked immunosorbent assay. All of treatment significantly reduced protein level the each marker with a statistical difference compared with saline treatment (analysis of variance [ANOVA], $p < .0001$; *, Tukey post hoc test at $p < .05$ with saline). Additionally, CM, HPSC, and CM + PRP treatment significantly reduced cystatin C **(C)** and caspase-3 protein **(D)** compared with that of PRP treatment (ANOVA, $p < .0001$; *, Tukey post hoc test at $p < .05$; *, with saline; **, with PRP). Abbreviations: AMC, age-matched control; CM, conditioned medium; HPSC, human placental stem cell; NGAL, neutrophil gelatinase-associated lipocalin; PRP, platelet-rich plasma.

The results include antiapoptotic effects (Figs. 2C, 2D, 2G, 2H, 6B) and proproliferation of renal and endothelial cells (Figs. 1–2A, 2B, 2E, 2F, 6A; Supporting Information Figs. S1–S3) with maintaining the renal cell phenotype (Supporting Information Fig. S4). To better understand the potential mechanisms involved in the therapeutic effect of HPSC-CM, we analyzed the growth factors and cytokines in the CM. The protein levels of follistatin, uPAR, ANGPTL4, HGF, and VEGF were higher in the HPSC-CM (Supporting Information Fig. S7) than other factors. Interestingly, studies have shown that individual administration of follistatin [33], HGF [34], or VEGF [35] is effective in accelerating tubular regeneration in animals with renal I/R. Follistatin treatment, through blocking activins or transforming growth factor-beta superfamily members, reduced renal injury by I/R [33]. The combination of VEGF and HGF or ANGPTL4 [36, 37] was reported to improve angiogenic response of tissues. Moreover, uPAR was also suggested as a crucial factor in VEGF-mediated endothelial cell migration [38]. Thus, it is plausible that various growth factors and cytokines secreted from HPSCs act in concert to attenuate renal injury and promote kidney repair after I/R. In the future study, it remains to be seen whether combinational treatment with the identified factors would result in a similar or better renal regeneration than that observed in the CM delivered group.

As discussed earlier [11, 32], the improvement or maintenance of angiogenic activities by CM treatment seems to be a critical factor to explain the restoration of kidney injury. The PTC rarefaction index (Supporting Information Fig. S6A) results indicate that the efficient delivery of CM using PRP (CM + PRP) facilitated to maintain similar level of angiogenesis observed in the normal kidney (AMC), whereas other experimental groups did not maintain intact angiogenic capability. In an attempt to explain the functional angiogenic ability, we focused on VEGF, which has been implicated as a vital factor for kidney repair following I/R via its mitogenic, angiogenic, anti-inflammatory, and anti-apoptotic effects [35]. As the CM contains high levels of VEGF in the components (Supporting Information Fig. S7), positive outcomes in the angiogenesis may be because of the exogenously injected CM. Interestingly, the highest protein level of endogenous VEGF in kidney tissues was detected in the CM-PRP group (Supporting Information Fig. S6B). We suggest that CM delivery can activate endogenous molecular systems in the injured kidney that contribute to renal improvement. As renal tubules are significant sources of VEGF and the angiogenic effects of tubular VEGF are essential for the preservation and maintenance of PTC integrity [39, 40], positive feedback between the attenuation of PTC rarefaction and increased VEGF signaling attenuated renal injury after I/R.

Several issues still need to be addressed to obtain better therapeutic outcomes. First, a more careful strategy for selecting the CM delivery vehicle is needed. We used a PRP gel system as a CM delivery vehicle, considering it as a

potential autologous source for patients. PRP gel as an autologous hydrogel system has been safely applied in preclinical and clinical studies for accelerating tissue repair [41, 42] [43–45]. In our study, the results of serum Cr and NAGL (Fig. 4) showed that a single application of PRP in our renal injury model was not able to improve renal function, which was similar to that of saline administration. However, the level of renal damage markers in the kidney tissue harvested at 7 days post-treatment significantly reduced in the PRP treatment group compared with that in the saline (Fig. 4). These results indicate positive effects of the PRP treatment on the renal functions. Conversely, Martin-Sole et al. [46] recently reported opposite results, where PRP treatment worsened renal blood flow and caused more renal histologic damage in rats with I/R. The authors suggested early thrombus formation, high osmolality of PRP, and the role of inflammatory cytokines from PRP as possible causes. In their report [46], the authors injected 1 ml of PRP solution to a left kidney, whereas our study used 20 µl for the injections into two kidneys. It can be considered that the significant difference in the injection volume may be a critical reason for the discrepancy in the results. As such, optimization of the PRP volume and number should be determined for clinical application. Alternatively, clinically relevant hydrogel systems such as collagen or fibrin gel are another candidates for delivery vehicles [47].

Conclusion

To the best of our knowledge, this is the first study to demonstrate the beneficial effects of physical encapsulation of stem cell-derived CM on kidney repair. For clinical applications of CM using PRP, standardized methods of production and validation of its use need to be conducted. Future work also should elucidate if CM with PRP can block the transition from AKI to CKD.

Acknowledgments

We thank the Regenerative Medicine Clinical Center at Wake Forest Institute for Regenerative Medicine for the HPSC and also acknowledge the editorial work of Karen Klein, M.A., in the Wake Forest Clinical and Translational Science Institute (UL1 TR001420; PI: McClain), as well as Dr. Weling Zhao. This study was supported, in part, by a grant from the State of North Carolina.

Author Contributions

H.E.Y: collection and/or assembly of data, data analysis and interpretation, manuscript writing; D.S.K., H.C.C., B. S., M.W.K., Z. A., J.H.K.: collection and/or assembly of data, data analysis and interpretation; K.H.M. and S.K.G.: conception/design; I.K. K: conception/design, collection and/or assembly of data, data analysis and interpretation, manuscript writing; J.J.Y.: conception/design, final approval of manuscript.

Disclosure of Potential Conflicts of Interest

The authors indicated no potential conflicts of interest.

References

1 Siew ED, Davenport A. The growth of acute kidney injury: A rising tide or just closer attention to detail? Kideny Int 2015;87: 46–61.

2 Rewa O, Bagshaw SM. Acute kidney injury-epidemiology, outcomes and economics. Nat Rev Nephrol 2014;10:193–207.

3 Lee PY, Chien Y, Chiou GY et al. Induced pluripotent stem cells without c-Myc attenuate acute kidney injury via downregulating the signaling of oxidative stress and inflammation in ischemia-reperfusion rats. Cell Transplant 2012;21:2569–2585.

4 Barnes CJ, Distaso CT, Spitz KM et al. Comparison of stem cell therapies for acute kidney injury. Am J Stem Cell 2016;5:1–10.

5 Chung HC, Ko IK, Atala A et al. Cell-based therapy for kidney disease. Korean J Urol 2015;56:412–421.

6 Herberts CA, Kwa MS, Hermsen HP. Risk factors in the development of stem cell therapy. J Transl Med 2011;9:29.

7 Pawitan JA. Prospect of stem cell conditioned medium in regenerative medicine. Biomed Res Int 2014;2014:965849.

8 Togel F, Hu Z, Weiss K et al. Administered mesenchymal stem cells protect against ischemic acute renal failure through differentiation-independent mechanisms. Am J Physiol Renal Physiol 2005;289:F31–F42.

9 Togel F, Weiss K, Yang Y et al. Paracrine actions of infused mesenchymal stem cells are important to the recovery from acute kidney injury. Am J Physiol Renal Physiol 2007;292:F1626–F1635.

10 Tarng DC, Tseng WC, Lee PY et al. Induced pluripotent stem cell-derived conditioned medium attenuates acute kidney injury by downregulating the oxidative stress-related pathway in ischemia-reperfusion rats. Cell Transplant 2016;25:517–530.

11 van Koppen A, Joles JA, van Balkom BW et al. Human embryonic mesenchymal stem cell-derived conditioned medium rescues kidney function in rats with established chronic kidney disease. PLoS One 2012;7:e38746.

12 Xing L, Cui R, Peng L et al. Mesenchymal stem cells, not conditioned medium, contribute to kidney repair after ischemia-reperfusion injury. Stem Cell Res Ther 2014;5:101.

13 Abedi A, Azarnia M, Jamali Zahvarehy M et al. Effect of different times of intraperitoneal injections of human bone marrow mesenchymal stem cell conditioned medium on gentamicin-induced acute kidney injury. Urol J 2016;13:2707–2716.

14 Khosravi A, Cutler CM, Kelly MH et al. Determination of the elimination half-life of fibroblast growth factor-23. J Clin Endocrinol Metab 2007;92:2374–2377.

15 Zern BJ, Chu H, Wang Y. Control growth factor release using a self-assembled [polycation:heparin] complex. PLoS One 2010;5:e11017.

16 Richardson TP, Peters MC, Ennett AB et al. Polymeric system for dual growth factor delivery. Nat Biotech 2001;19:1029–1034.

17 Chen FM, Zhang M, Wu ZF. Toward delivery of multiple growth factors in tissue engineering. Biomaterials 2010;31:6279–6308.

18 Ko IK, Ju YM, Chen T et al. Combined systemic and local delivery of stem cell inducing/recruiting factors for in situ tissue regeneration. FASEB J 2012;26:158–168.

19 Patel AN, Selzman CH, Kumpati GS et al. Evaluation of autologous platelet rich plasma for cardiac surgery: Outcome analysis of 2000 patients. J Cardiol Surg 2016; 11:62.

20 Li W, Enomoto M, Ukegawa M et al. Subcutaneous injections of platelet-rich plasma into skin flaps modulate proangiogenic gene expression and improve survival rates. Plast Reconstr Surg 2012;129:858–866.

21 Oliveira MS, Barreto-Filho JB. Placental-derived stem cells: Culture, differentiation and challenges. World J Stem Cell 2015;7: 769–775.

22 Hao Y, Ma DH, Hwang DG et al. Identification of antiangiogenic and anti-inflammatory proteins in human amniotic membrane. Cornea 2000;19:348–352.

23 Liu SH, Huang JP, Lee RK et al. Paracrine factors from human placental multipotent mesenchymal stromal cells protect endothelium from oxidative injury via STAT3 and manganese superoxide dismutase activation. Biol Reprod 2010;82:905–913.

24 Zhang K, Guo X, Li Y et al. Electrospun nanoyarn seeded with myoblasts induced from placental stem cells for the application of stress urinary incontinence sling: An

in vitro study. Colloid Surf B Biointerfaces 2017;105:1986–2000.

25 Skardal A, Murphy SV, Crowell K et al. A tunable hydrogel system for long-term release of cell-secreted cytokines and bioprinted in situ wound cell delivery. J Biomed Mater Res B Appl Biomater 2016;105:1986–2000.

26 George SK, Abolbashari M, Jackson JD et al. Potential use of autologous renal cells from diseased kidneys for the treatment of renal failure. PLoS One 2016;11:e0164997.

27 Landesberg R, Burke A, Pinsky D et al. Activation of platelet-rich plasm using thrombin receptor agonist peptide. J Oral Maxillofac Surg 2005;63:529–535.

28 Yamaleyeva LM, Guimaraes-Souza NK, Krane LS et al. Cell therapy with human renal cell cultures containing erythropoietin-positive cells improves chronic kidney injury. Stem Cells Translational Medicine 2012;1: 373–383.

29 Kang DH, Joly AH, Oh SW et al. Impaired angiogenesis in the remnant kidney model: I. Potential role of vascular endothelial growth factor and thrombospondin-1. J Am Soc Nephrol 2001;12:1434–1447.

30 McIlroy DR, Wagener G, Lee HT. Biomarkers of acute kidney injury: An evolving domain. Anesthesiology 2010;112:998–1004.

31 Guo R, Wang Y, Minto AW et al. Acute renal failure in endotoxemia is dependent on caspase activation. J Am Soc Nephrol 2004; 15:3093–3102.

32 Overath JM, Gauer S, Obermuller N et al. Short-term preconditioning enhances the therapeutic potential of adipose-derived stromal/stem cell-conditioned medium in cisplatin-induced acute kidney injury. Exp Cell Res 2016;342:175–183.

33 Fang DY, Lu B, Hayward S et al. The role of activin A and B and the benefit of follistatin treatment in renal ischemia-reperfusion injury in mice. Transplant Direct 2016;2:e87.

34 Miller SB, Martin DR, Kissane J et al. Hepatocyte growth factor accelerates recovery from acute ischemic renal injury in rats. Am J Physiol 1994;266:F129–F134.

35 Mori da Cunha MG, Zia S, Beckmann DV et al. Vascular endothelial growth factor up-regulation in human amniotic fluid stem cell enhances nephroprotection after ischemia-reperfusion injury in the rat. Crit Care Med 2017;45:e86–e96.

36 Sulpice E, Ding S, Muscatelli-Groux B et al. Cross-talk between the VEGF-A and HGF signalling pathways in endothelial cells. Biol Cell 2009;101:525–539.

37 Hu K, Babapoor-Farrokhran S, Rodrigues M et al. Hypoxia-inducible factor 1 upregulation of both VEGF and ANGPTL4 is required to promote the angiogenic phenotype in uveal melanoma. Oncotarget 2016;7: 7816–7828.

38 Alexander RA, Prager GW, Mihaly-Bison J et al. VEGF-induced endothelial cell migration requires urokinase receptor (uPAR)-dependent integrin redistribution. Cardiovasc Res 2012;94:125–135.

39 Lin SL, Chang FC, Schrimpf C et al. Targeting endothelium-pericyte cross talk by inhibiting VEGF receptor signaling attenuates kidney microvascular rarefaction and fibrosis. Am J Pathol 2011;178:911–923.

40 Basile DP, Friedrich JL, Spahic J et al. Impaired endothelial proliferation and mesenchymal transition contribute to vascular rarefaction following acute kidney injury. Am J Physiol Renal Physiol 2011;300: F721–F733.

41 DeRossi R, Coelho AC, Mello GS et al. Effects of platelet-rich plasma gel on skin healing in surgical wound in horses. Acta Cir Bras 2009;24:276–281.

42 Carter CA, Jolly DG, Worden CE et al. Platelet-rich plasma gel promotes differentiation and regeneration during equine wound healing. Exp Mol Pathol 2003;74:244–255.

43 Mafi A, Dehghani F, Moghadam A et al. Effects of platelet-rich plasma on liver regeneration in CCl4-induced hepatotoxicity model. Platelets 2016;27:771–776.

44 Zhang Y, Ying G, Ren C et al. Administration of human platelet-rich plasma reduces infarction volume and improves motor function in adult rats with focal ischemic stroke. Brain Res 2015;1594:267–273.

45 Bakacak M, Bostanci MS, Inanc F et al. Protective effect of platelet rich plasma on experimental ischemia/reperfusion injury in rat ovary. Gynecol Obstet Invest 2016;81: 225–231.

46 Martin-Sole O, Rodo J, Garcia-Aparicio L et al. Effects of platelet-rich plasma (PRP) on a model of renal ischemia-reperfusion in rats. PLoS One 2016;11: e0160703.

47 Calo E, Khutoryanskiy VV. Biomedical applications of hydrogels: A review of patents and commercial products. Eur Polym J 2015; 65:252–267.

See www.StemCellsTM.com for supporting information available online.